NEUTRAL HYDROGEN AT HIGH REDSHIFTS AS A PROBE OF STRUCTURE FORMATION: 1.POST COBE ANALYSIS OF CDM AND HDM MODELS

K. Subramanian[1] and T. Padmanabhan[2*]

[1]National Centre for Radio Astrophysics, TIFR
Poona University Campus, Ganeshkind, Pune 411007, India.
email:kandu@gmrt.ernet.in

[2] Inter University Center for Astronomy and Astrophysics,
Poona University Campus, Ganeshkind, Pune 411007, India.
email:paddy@iucaa.ernet.in

ABSTRACT

The structures which form in the universe at redshifts $z \lesssim 10$ can be detected and studied using the redshifted 21 cm line emission from the neutral hydrogen. We compute the expected co-moving number density, N, of protocondensates which will emit a flux higher than S, at various redshifts, in the CDM and HDM models. The models are normalised using the COBE results. Our results are compared with the present and expected sensitivities of various telescopes for the detection of protocondensates. In the CDM models the predicted maximum fluxes at a redshift $z \simeq 3.3$, are about $(1.5 - 3)$ mJy and $N \simeq (10^{-8} - 10^{-7}) Mpc^{-3}$. These protocondensates cannot be detected with the present sensitivities but will become detectable in the near future with improved sensitivity. At lower redshifts, the detectability of these structures critically depends on their neutral hydrogen content. In the redshift range around $z \simeq 5$, *individual* protocondensates will not be detectable. However, the excess variance due to fluctuations with small density contrasts will be detectable with somewhat large (say, about 60 hours) integration time. At still higher redshifts, it would be virtually impossible to see any signal with even such large integration time. Biased CDM models predict larger fluxes, but somewhat lower abundances. Finally, the HDM models - when normalised using COBE - do *not* lead to detectable number of sources ('pancakes') at redshifts $z \gtrsim 2$.

IUCAA-19/92 Nov 92; submitted for publication

* On leave of absence from: TIFR, Homi Bhabha Road, Bombay 400 005

1. Introduction

It is generally believed that galaxies and other large scale structures in the universe originated by the growth of small initial perturbations via gravitational instability. If this picture is correct, then one should be able to see some signature of the protocondensates in the universe at a redshift range of, say, $z \lesssim 10$ or so. Sunayaev and Zeldovich (1972, 1974) first pointed out that the birth of the large scale structures could possibly be probed by observing the (redshifted) 21 cm line emitted by neutral hydrogen in the incipient galaxies and clusters. If such radiation is detected it could open up an entirely new window to the high redshift universe.

Several searches have been made so far at meter wavelengths for the redshifted 21 cm line. Many of these searches had only yielded null results (cf. Subrahmanyan and Swarup 1990, Subrahmanyan and Anantharamaiah 1990, Uson et. al 1991a, Wieringa et. al 1992 and references cited therein). Recently, however, Uson et al. (1991b) have claimed the first ever detection of a neutral hydrogen rich protocluster at $z = 3.4$. The Gaint Meterwave Radio Telescope (GMRT) presently being constructed in India - and expected to go into operation by 1994 - should be able to improve the observational situation considerably as regards detection and study of protocondensates containing neutral hydrogen (Swarup 1984). It is, therefore, interesting to work out the expected flux of redshifted 21 cm emission in various models of structure formation and compare the results with both the present observational limits and the expected sensitivity limits of future instruments like GMRT.

The expected properties of 21 cm emission from protoclusters depends sensitively on the theory of galaxy formation. While several authors have studied (Sunyaev and Zeldovich 1974, Hogan and Rees 1979, Subrahmanyan 1989, Scott and Rees 1990, Subramanian and Swarup 1992) this issue in the past, a comprehensive analysis of the of this problem, taking into account different models for structure formation has not yet been done. This is the first of a series of papers addressing this question. Here we work out the expected number density of protocondensates in the CDM and HDM models. Future papers will address the details of the line profile, expected pattern of sky brightness and the detailed ionisation history of the universe.

Definitive predictions about the 21 cm emission could not be made in the past because of the following crucial difficulty. Theories of structure formation are usually specified by giving the power spectrum of density fluctuations, upto a normalisation constant. Until recently this normalisation constant was an unknown parameter, introducing a major ambiguity in the predicted flux of 21 cm emission. Recently, however, the COBE satellite has detected (Smoot et al, 1992) temperature anisotropies of the cosmic microwave background radiation (CMBR). Using the COBE results, one can unambiguously fix the normalisation constant in the power spectrum of any specific model. This reduces the uncertainty in theoretical models to a great extent and allows us to perform a more reliable calculation.

This paper is organised as follows: In the next section, we will discuss the possible sources of 21 cm line emission in the universe and some details regarding the observational procedures. In section 3, which forms the core of the paper, we will derive the detailed properties of these sources in the CDM model. These results are presented in terms of the expected number $N(S)$ of sources emitting flux larger than some value S. We calculate $N(S)$ for different redshifts and for range of values of the parameters in the problem. Section 4 describes why the HDM models do not perform as well as the CDM models when both are normalised properly using the COBE results. The last section presents a short summary of the paper.

2.Neutral hydrogen at high redshifts: sources and detection

A 21 cm (or, equivalently, a 1420 MHz) photon is emitted when a hydrogen atom makes a transition from a state in which the electron and proton spins are aligned to a state in which the spins are anti-aligned. It is usual to define an effective 'spin' temperature T_s by the relation $n(\mathrm{up})/n(\mathrm{down}) = \exp(-\Delta E/kT_s)$ where $n(\mathrm{up})$ etc. denotes the population of the upper level and ΔE is the energy difference between the levels. The relative magnitude of T_s with respect to the background radiation temperature, T_b, will then decide whether absorption or emission will be the dominant effect in a given cloud of neutral hydrogen; a cloud will be seen in emission if $T_s > T_b$ and in absorption if $T_s < T_b$. Scott and Rees (1990) have examined this issue in detail for several models for structure formation and have concluded that $T_s > T_b$ in most likely situations. We will also be mostly dealing with cases in which the neutral hydrogen structure shows up in emission.

Further, in all the cases we consider the optical depth of the hydrogen cloud to the 21 cm photons is quite small. Hence, one can calculate the flux in the emission line by adding the photons emitted by each hydrogen atom in the cloud. It can be shown that (see eg. Spitzer, 1976) the peak flux density (S_ν) of the 21 cm line radiation, from an optically thin cloud containing neutral hydrogen of mass M_{HI}, is

$$S_\nu = 5.3 mJy \left(\frac{M_{HI}}{10^{13} M_\odot}\right) \left(\frac{\Delta\nu_o}{1 MHz}\right)^{-1} \left[\frac{\Omega_0^4 h^2}{(\Omega_0 z + (\Omega_0 - 2)((1+\Omega_0 z)^{1/2} - 1))^2}\right] \qquad (1)$$

Here $\Delta\nu_0$ is the frequency width (FWHM for a Gaussian profile) of the observed emission line, z is the redshift of the cloud, Ω_0 the density parameter of the universe, and h is the Hubble constant in units of 100 $kms^{-1}Mpc^{-1}$. The frequency width can be related to the velocity width (Δv) of the cloud by $(\Delta\nu_0/\nu_0) = (\Delta v/c)$; that is,

$$\Delta\nu_0 = \frac{4.7}{1+z} MHz \left(\frac{\Delta v}{1000 kms^{-1}}\right) \qquad (2)$$

Thus the peak flux density (which we shall hereafter call just 'flux') can be computed if the mass of the neutral hydrogen and the velocity dispersion are known. As we shall see later, the velocity dispersion can be obtained from the gravitational dynamics of the cloud; the *total* mass of the cloud can also be related to various other known quantities in the problem. The mass of the *neutral* hydrogen contained in the cloud needs now to be related to the total mass. To do this, we have to take into account the fact that existing observations of quasars at high redshifts already constrain the neutral hydrogen content of the universe at $z \lesssim 5$.

Firstly, the absence of any (Gunn-Peterson) dip in the ultraviolet spectra of quasars, shortward of the Ly α emission line, suggests that any smoothly distributed hydrogen in the universe is likely to be almost completely ionised at $z \lesssim (4-5)$ (Gunn and Peterson 1965, Miralda-Escude and Ostriker 1990). It is, however, possible to regenerate neutral hydrogen from the inter galactic medium (IGM) during gravitational collapse, provided the gas can cool efficiently. In the hierarchical models for structure formation, this is expected to happen on subgalactic scales first and on larger scales progressively later. [In the HDM model - in which cluster mass scales collapse first to form pancake-like structures - a significant fraction of the hydrogen will become neutral as the gas in the dense pancake cools. This was indeed the major source of neutral hydrogen discussed in the original papers of Sunyaev and Zeldovich. We will see later that this model - unfortunately - fails to produce detectable signal. The reason has to do with the COBE results which has now fixed the normalisation constant in the spectrum uniquely; see section 5.]

Secondly, although quasar spectra do not show the Gunn-Peterson dip due to smoothly distributed HI, they do exhibit many HI absorption lines, indicating the existence of neutral hydrogen in clumped form. The damped Lyα systems are particularly interesting in

the present context (Wolfe et al., 1986; Wolfe, 1989; Turnshek et al., 1989; Lanzetta et al.,1991). These absorbers contain, at their observed redshift of $z \sim (2-4)$, as much mass in neutral hydrogen as the total stellar content of all present day disk galaxies. In fact, Wieringa et al. (1992) make the interesting point that the observed abundance of these systems may also be consistent with a scenario in which the bulk of the precursors of rich clusters are still neutral at the redshifts of $z \simeq (2-4)$.

The above considerations suggest that we should focus on the emission from the clumps or collection of clumps - revealed by, for example, the absorption lines in quasar spectra - if we want to detect HI at $z \lesssim 5$,. This will be of relevance in what follows.

In the following sections we will consider different models of galaxy formation and work out the expected flux of line emission from neutral hydrogen at several redshifts. While these results can be computed - in principle - for any redshift, it is certainly more useful to concentrate on the redshifts which are being directly probed by the existing and future instruments. One of the frequency bands which is currently being used by several groups is around 327 MHz, corresponding to a redshift of $(1420/327) - 1 = 3.34$. A significant part of this paper is devoted to working out the expected line emission from sources at this redshift. The GMRT will also be able to probe several other frequency bands around 610 MHz, 233 MHz and 150 MHz, corresponding to redshifts of 1.33, 5.1 and 8.47 respectively. We shall also examine the expected 21 cm flux from these epochs.

The actual search for 21 cm flux generally proceeds in the following manner: One uses a fourier-synthesis telescope consisting of both a compact array of antennas and an extended array. The extended array is used to make a high resolution image of the continuum emission over the field of view. This is then subtracted from the data acquired by the compact array leaving behind the line emission in the presence of noise. The resulting data can be smoothed to various angular ($\Delta\theta$) and frequency ($\Delta\nu$) resolutions to produce a spectral line data cube. (There will, of course, be a minimum $\Delta\theta$ defined by the synthesized beam size, θ_s, and a minimum frequency resolution which can be attained by a given telescope.) The spectral-line-cube samples a comoving volume of space whose two dimensions are defined by the area covered by the primary beam and whose depth is proportional to the total frequency bandwidth. The cube itself is made up of pixels defined by $\Delta\theta$ and $\Delta\nu$. The choice of $\Delta\theta$ is governed by the desire to maximise the signal-to-noise ratio. If one chooses too small a $\Delta\theta$, then only part of the source will be observed in each pixel and signal will be small. On the other hand if $\Delta\theta$ is taken to be so large such that there are few antenna pairs with correspondingly small baselines, noise will increase. Hence, ideally, the instrumental resolution has to match the angular size of the protocluster. Similarly $\Delta\nu$ is chosen so that the noise is minimised and at the same time the emission line spans over a width of at least $\Delta\nu$.

The spectal-line-cube can be analysed in two different ways to see if there are signals of 21 cm emission. Firstly, one can look for correlated pixels which have much higher levels of flux than the rms noise (σ_N) per pixel. Typically, one would look for pixels with a peak flux greater than 5 σ_N above the noise. Secondly one can see if there is an excess variance in the flux per pixel, over and above the noise. The first mode is useful for detecting isolated luminous objects, while the second method may be useful in picking out an inhomogeneous (but not highly over dense) distribution of neutral hydrogen. We shall mostly deal with the predictions for the first type of signal and will comment on the second approach whenever relevant. The main question, therefore, is the following: Given a detection system (like, say, GMRT) operating at a set of frequency bands and some model for the structure formation, what is the abundance of objects emitting a flux higher than, say, n times the rms noise level of the instrument ? We shall now take up this issue, beginning with the Cold Dark Matter (CDM) model for structure formation.

3. The 21 cm flux in CDM model

3.1 Preliminary considerations

In the CDM model for the galaxy formation the universe is dominated by dark matter particles with negligible random velocities. It is usual to assume that the primordial density field is a random Gaussian variable with a power spectrum of the Harrison - Zeldovich form: $P(k) = Ak$. The power spectrum at sufficiently late epochs - say, just after recombination - is well approximated by the fitting function: (Peebles 1983, Davis et. al. 1985)

$$P(k) = \frac{Ak}{(1 + Bk + Ck^{3/2} + Dk^2)^2} \tag{3}$$

with $B = 1.7(\Omega_0 h^2)^{-1}$ Mpc, $C = 9(\Omega_0 h^2)^{-3/2} Mpc^{3/2}$ and $D = 1(\Omega_0 h^2)^{-2} Mpc^2$. The shape of the power spectrum is completely specified by the dynamics while the amplitude A can now be fixed by comparing the quadrapole anisotropy in MBR produced by this spectrum with the observed COBE result. Such an analysis (see eg., Padmanabhan and Narasimha, 1992) gives the value $A = [(24 \pm 4)\mathrm{h}^{-1}\ \mathrm{Mpc}]^4$. We shall use the value $A = [24\mathrm{h}^{-1}\ \mathrm{Mpc}]^4$ unless mentioned otherwise.

The mean-square-fluctuation $\sigma^2(R) =< (\delta M/M)^2_R >$ in the mass contrast within a sphere of radius R, placed randomly somewhere in the universe can be related to $P(k)$ by

$$\sigma^2(R) = \int_0^\infty \frac{dk}{k} \left(\frac{k^3 P(k)}{2\pi^2}\right) \left[\frac{3(\sin kR - kR\cos kR)}{(kR)^3}\right]^2 \tag{4}$$

We show in figure 1 a plot of $\sigma(R)$ for the CDM power spectrum, linearly extrapolated to the present epoch, adopting COBE normalisation. One sees that $\sigma(R)$ is fairly flat at small subgalactic scales, decreases gently with R and falls of asymptotically as $\sigma \simeq (R_0/R)^2$ with $R_0 \simeq 24\mathrm{h}^{-1}$ Mpc. Since $\sigma(R)$ is a (gently) decreasing function of R, small mass scales will collapse first in this model. Structures will form hierarchically with larger mass scales going nonlinear at later times. Since a sphere of comoving radius R will contain a mean mass of $M(R) = (4\pi/3)\rho_0 R^3$ (where ρ_0 is the mass density of the universe at present), we can also treat σ as a function of the mass scale: $\sigma(M) = \sigma[R(M)]$. In what follows, we shall use either form depending on the convenience.

The functions $P(k)$,$\sigma(R)$ and $\sigma(M)$can always be approximated locally by a power law: if $P(k) \propto k^n$ then $\sigma \propto R^{-(n+3)/2} \propto M^{-(n+3)/6}$; the effective index n is (-3) at small scales and increases to 1 at large scales. At $M \simeq 10^9 M_\odot$, $n = -2.3$, at $M \simeq 10^{12} M_\odot$, $n = -2$ and at $M \simeq 10^{15} M_\odot$, $n = -1$.

Given $\sigma(M)$ one can estimate the redshift z_{coll}, at which a mass scale M collapses and forms a bound object. Consider, for example, a spherical region of radius R containing a density contrast $\delta_0(R)$ which is n times the variance $\sigma(R)$ at that scale. The standard spherical model (see eg., Peebles, 1980) then leads to an estimate:

$$(1 + z_{coll}) = \frac{\delta_0(R)}{1.686} = \frac{n\sigma(R)}{1.686} \tag{5}$$

(We stress the convention that $\delta_0(R)$ is the average excess density contrast in a sphere of radius R, linearly extrapolated to the present epoch.) With COBE normalisation, typical (i.e, 1σ) regions containing cluster scale masses ($10^{14} M_\odot$) collapse only at low redshifts,

$z \simeq 0.35$; even a 4σ fluctuation at the cluster scales - which has a relative probability of $\exp(-8) \simeq 3.35 \times 10^{-4}$ - at cluster scale collapses only at $z \simeq 4.4$. So at the redshifts probed by various HI searches, protoclusters could *not* have collapsed and virialised in the CDM models (We shall see in section 5 that the situation is worse for HDM models). From the constraints discussed in the previous section, it follows that the gas which is *smoothly distributed* within the protocluster will *not* be neutral for $z \lesssim 5$.

There is, however, another source for neutral hydrogen in these models (eg. Subramanian and Swarup 1992). Note that, in the CDM picture, smaller mass scales do have a large enough σ for them to collapse at high redshifts; hence the gas which has collapsed into these small mass scale objects could cool and form neutral clumps of hydrogen. A region of the size of a protocluster will then consist of many small scale clumps containing neutral hydrogen, provided the ionisation processes are not sufficiently effective. The photons constituting the metagalactic UV flux and the UV photons emitted during the formation of massive stars could play a possible role in ionising the gas in these clumps. The metagalactic flux is so efficient in heating the gas in small clumps ($M \lesssim 10^9 M_\odot$) that they do not collapse in the first place (eg. Efstathiou 1992). But for larger masses, such heating cannot prevent the collapse of the gas. In this case, the gas in the clumps becomes dense enough to prevent significant ionisation by the metagalactic UV photons. As for as star formation is concerned, the degree of ionisation depends crucially on the rate of star formation R. Unfortunately R is not known with any degree of precision. However one can put some limits on R, at least in the case of the damped Lyα systems; these limits suggest that R cannot be so large as to ionise the gas in a young galaxy significantly, at least as long as it has not converted the bulk of its gas into stars (Cowie, 1988; Subramanian and Swarup, 1992). Assuming that the clumps we are considering are similar in structure to the damped Lyman alpha systems seen at high redshifts, we could expect the gas to be neutral at these redshifts in spite of star formation. These clumps can be a significant source for the 21 cm flux from such a protocluster. We shall now estimate this flux.

3.2 Flux from the clumps in a protocondensate

For calculating the flux we have to first estimate the fraction of the gas in a protocluster (f_{coll}), which is in the form of collapsed objects, at any particular redshift. Of this, a further fraction, say f_N, will be in the form of HI. Suppose $f(M,z)dM$ is the number density of collapsed objects at a redshift z within a mass range M and $M + dM$. Let us assume that the gas in a collapsed object can cool efficiently if it has a mass in the range $M_1 < M < M_2$. From the usual cooling arguments applied to the CDM model (cf. Blumenthal et al. 1984, Efstathiou 1992), one can estimate that $M_1 \simeq 10^9 M_\odot$ and $M_2 \simeq 10^{12} M_\odot$. In that case, the mass of HI contained in the small scale objects populating a protocluster of proper volume V and excess density contrast $\delta(z)$ is

$$M_{HI} = f_N f_b \int_{M_1}^{M_2} M f(M,z) dM \times V \times (1 + \delta(z)). \tag{6}$$

where f_b is the fraction of the mass in the universe which is in the form of baryons. In practice, we will take V to be the volume of a sphere of radius l, where l is related to the angular resolution $\Delta\theta$ of the telescope by the equation:

$$\begin{aligned} \Delta\theta &= l(1+z)^2 \frac{H_0}{2c} \left[\frac{\Omega_0^2}{(\Omega_0 z + (\Omega_0 - 2)((1+\Omega_0 z)^{1/2} - 1))} \right] \\ &\approx 0.57 \mathrm{arcmin} h \frac{1+z}{[1-(1+z)^{-1/2}]} \left(\frac{l}{1Mpc} \right); \quad \text{for } \Omega_0 = 1 \end{aligned} \tag{7}$$

[This is the standard relation between the proper length at a redshift z and the angle it subtends at the observer].

An estimate of $f(M,z)$ can be obtained from the hierarchical clustering theory of Press and Schecter (1974). Using the Press-Schecter formula for the mass function of collapsed objects we get

$$\int_{M_1}^{M_2} Mf(M,z)dM = -\int_{M_1}^{M_2} M[\frac{\bar{\rho}}{M}(\frac{dF}{dM})]dM = \bar{\rho}(z)[F(M_1) - F(M_2)] = \bar{\rho}(z)f_{coll}(z), \tag{8}$$

where

$$F = \mathrm{erfc}[\frac{\delta_c(t,t_i)}{\sqrt{(2)}\sigma(R,t_i)}] = \mathrm{erfc}[\frac{1}{\sqrt{2}}(\frac{M}{M_{nl}})^{(3+n)/6}] \tag{9}$$

In the above equation, $\delta_c(t,t_i)$ is the critical excess density contrast needed at time t_i so that the fluctuation collapses at time t; $\sigma(R,t_i) = \sigma(R)/(1+z_i)$ and erfc is the complementary error function defined by

$$\mathrm{erfc}(x) = \frac{2}{\sqrt{\pi}}\int_x^\infty dt\ \exp(-t^2) \tag{10}$$

In arriving at the last equality in the equation (9) , we have used the (local) power law approximation $P(k) \propto k^n$, and expressed the results in terms of the mass scale $M_{nl}(z)$ which is collapsing at redshift z. This mass can be estimated from the spherical model by solving the (implicit) equation $\sigma[R(M_{nl})] = 1.686(1+z)$, where $R(M) = (3M/4\pi\rho_0)^{1/3}$ and ρ_0 is the cosmological density at present. (For example, the redshift 3.34 corresponds to $M_{nl} \approx 3 \times 10^{11} M_\odot$; the values of M_{nl} for several relevant redshifts are given in Table 1; b is the bias parameter, to be discussed in section 3.4)

Table 1 : The nonlinear masses and collapsed fractions at various z

redshift	b=1.0		b=1.5	
z	M_{nl}	f_{coll}	M_{nl}	f_{coll}
1.33	$8.6 \times 10^{12} M_\odot$	0.2354	$1.04 \times 10^{12} M_\odot$	0.3388
3.34	$2.9 \times 10^{11} M_\odot$	0.3822	$2.3 \times 10^{10} M_\odot$	0.4283
5.1	$3.4 \times 10^{10} M_\odot$	0.4265	$2.0 \times 10^{9} M_\odot$	0.3531
8.47	$1.3 \times 10^{9} M_\odot$	0.327	–	–

Writing the volume V as $(4\pi/3)l^3$ (where l is a *proper* radius) we can express the neutral hydrogen mass as

$$\begin{aligned} M_{HI} &= \bar{M}_{HI} \times (1+\delta(z)) = f_N f_b f_{coll}(z)\rho_0(1+z)^3 \times \frac{4\pi}{3}l^3 \times (1+\delta(z)) \\ &\approx 0.73 \times 10^{13} M_\odot h_{50}^2 \Omega_0 \left(\frac{f_N}{0.5}\right)\left(\frac{f_b}{0.1}\right)\left(\frac{f_{coll}}{0.5}\right)\left(\frac{l(1+z)}{10Mpc}\right)^3 [1+\delta(z)] \end{aligned} \tag{11}$$

where $h_{50} = (h/0.5)$. Substituting (2) and (11) in (1) we find that

$$S_{exp} = 0.202\ mJy\ \frac{h_{50}^4}{g(z)}\left(\frac{f_N}{0.5}\right)\left(\frac{f_b}{0.1}\right)\left(\frac{f_{coll}(z)}{0.5}\right)\left(\frac{l(1+z)}{10Mpc}\right)^3\left(\frac{\Delta v}{1000 Kms^{-1}}\right)^{-1}(1+\delta), \tag{12}$$

where Δv is the velocity width of the protocluster, $g(z) = (1+z)[1-(1+z)^{-1/2}]^2$ and we have set $\Omega_0 = 1$.

There is, however, one further complication which needs to be accounted for. This expression gives the flux from a region with density $\bar{\rho}(1+\delta)$ and velocity Δv. The uniform background will, of course, contribute an amount proportional to $(\bar{\rho}/\Delta v_H)$ where Δv_H is the velocity width due to the Hubble expansion across the radius of the protocluster. Since the observations look for a signal above the background, one has to subtract out the HI emission from the regions surrounding the protocluster. Hence the expected *signal* is proportional to

$$S_{sig} \propto \left[\frac{\bar{\rho}(1+\delta)}{\Delta v} - \frac{\bar{\rho}}{\Delta v_H}\right] \propto \left(\frac{\bar{\rho}(1+\delta)}{\Delta v}\right) f_{sig} \tag{13}$$

where the factor $f_{sig} = [1-(\Delta v)/(\Delta v_H(1+\delta))]$ takes into account the difference between the signal and background. Thus the final expression for the flux is

$$S_{sig} = S_{exp} \times f_{sig}. \tag{14}$$

The above subtlety makes very little difference to actual results when we have $1+\delta \gg 1$ and $\Delta v \ll \Delta v_H$, because in this case $f_{sig} \approx 1$. However if we are considering high redshifts at which $\delta \ll 1$, then we have to take account of the factor f_{sig}. In this linear regime of density contrast, we have $\Delta v \approx \Delta v_H(1-\delta/3)$ and $f_{sig} \approx 4\delta/3$.

Some of the scalings used in (14) deserve comment. Arguments based on big bang nucleosynthesis suggest that the baryonic fraction of the universe is about 0.1 (for $h = 0.5$) which is the value we have adopted. The fraction f_N of these baryons, which are in form of neutral hydrogen, is somewhat uncertain and its precise estimate requires detailed considerations of the thermal, ionisation and star formation histories of the gaseous component during the formation of the structures. This is subject of interest in its own right and we plan to address it in a future publication. In this work, we shall be content to take this number to be of order unity. This estimate should be valid at least for high redshifts, say $z \gtrsim 3$. A direct motivation for this assumption comes from the observations of the damped Ly α systems discussed in the previous section which show that the HI detected in these systems is comparable to the stellar content of all present day galaxies.

The other unknown quantities in (14) can all be estimated from the power spectrum (or $\sigma(R)$) and invoking some model for nonlinear evolution. We shall use here the spherical model to estimate the effects of non linear evolution. In this model, the density contrast $\delta(z)$ and velocity $v(z)$ at a redshift z is given by the (implicit) relations

$$1+\delta(z) = \frac{9}{2}\frac{(\theta-\sin\theta)^2}{(1-\cos\theta)^3} \tag{15}$$

$$1+z = \delta_0 \left(\frac{5}{3}\right)\left(\frac{4}{3}\right)^{2/3}(\theta-\sin\theta)^{-2/3} \tag{16}$$

$$v = \frac{2}{5}\left(\frac{5}{3}\right)^{3/2}\left(\frac{R}{t_0}\right)\delta_0^{1/2}\frac{\sin\theta}{1-\cos\theta} \approx 645.5\ Kms^{-1}\ \delta_0^{1/2} h_{50}\left(\frac{R}{10Mpc}\right)\frac{\sin\theta}{1-\cos\theta} \tag{17}$$

Here R is the *comoving* radius of the spherically overdense region which is related to the proper radius l by the mass conservation: $R = l(1+z)(1+\delta(z))^{1/3}$. The quantity δ_0 is related to the initial density contrast δ_i of the spherical region at some very early epoch z_i by

$$\delta_0 = (3/5)\delta_i(1+z_i) \tag{18}$$

In other words, δ_0 is the overdensity which the spherical region will have if the linear theory has been valid throughout the evolution. Equations (15) and (17) express δ and v in terms of the parameter θ (called 'evolution angle') which is related to the redshift by (16) . Often, it is convenient to rewrite (16) as

$$\delta_0 = 0.4953(1+z)(\theta - \sin\theta)^{2/3} \tag{19}$$

so that δ_0 is expressed in terms of the evolution angle and the redshift. Notice that the spherical model is parametrized by δ_0 and R.

The velocity width of the line Δv (defined as the FWHM in velocity space) will depend on the density profile of the protocluster. For our purpose, it is sufficient to approximate the density to be constant within l. Then the velocity of shells at different radii r depends linearly on r; in this case one can easily show that $\Delta v = \sqrt{2}v$. (For a centrally peaked density profile Δv is likely smaller than the above estimate.) Using equation (14) , (15) and (17) and substituting for Δv and $1+\delta(z)$ in terms of θ we then get for the flux

$$S = A(l,z)\left|\left[\frac{\theta - \sin\theta}{\sin\theta(1-\cos\theta)}\right]\right|, \tag{20}$$

where

$$A(l,z) = 0.857\, mJy\, h_{50}^3 \left(\frac{f_N}{0.5}\right)\left(\frac{f_b}{0.1}\right)\left(\frac{f_{coll}(z)}{0.5}\right)\left(\frac{l(1+z)}{10Mpc}\right)^2 f_{sig}\frac{(1+z)^{1/2}}{[1+z-\sqrt{(1+z)}]^2}. \tag{21}$$

The peak flux depends on z, l and the evolution angle θ which describes how far the protocluster has evolved towards collapse.

Note that, if $\delta \ll 1$, we can calculate the flux directly from the linear theory. In this case, we have

$$\Delta v = \sqrt{2}v_H(1-\frac{1}{3}\delta) \approx 707 kms^{-1}h_{50}(1+z)^{1/2}\left(\frac{l(1+z)}{10Mpc}\right) \tag{22}$$

where we have included a factor $\sqrt{2}$ in calculating the line width and set $f_{sig} = 4\delta/3$. Using these relations in (14) we get

$$S = 1.524\, mJy\, h_{50}^3 f_N \left(\frac{f_b}{0.1}\right) f_{coll}\left(\frac{l(1+z)}{10Mpc}\right)^2 \frac{\delta(z))}{(1+z)^{1/2}g(z)}. \tag{23}$$

In our expression (20) , the flux can increase to very high values if the velocity width Δv tends to zero. The following point, however, should be noted. The smaller scale structures in the protocluster (whose neutral hydrogen is contributing to our flux) will themselves have a velocity width, say $\Delta v_g \simeq 300 kms^{-1}$ for 'galactic' mass clumps. So even when the velocity dispersion of the large system falls below that of the constituents, the actual velocity width will still be dominated by that of the constituents. That is, when $\Delta v \lesssim \Delta v_g$ for the protocluster, we must set $\Delta v \simeq \Delta v_g$. We shall need this result later.

Consider now any observational project which is searching for the 21 cm line emission. The details of the instrument configuration will specify for us the values of l and z. [The value of l corresponds generally to the synthesized beam size θ_s that is employed in the observations (for which the sensitivity to the detection of HI emission is maximised),

although we will consider here a range of l about this value.] Once the redshift is specified, it is straightforward to calculate $M_{nl}(z)$ and use (9) to estimate f_{coll}. In table 1 we have also given the f_{coll} estimated for a number of redshifts relevant to the present and planned EI observations. All the quantities in equation (21) are now known except θ, which is uniquely related to δ_0 once z is fixed (see equation (19)). Given the value of δ_0 we can compute S.

In the standard CDM model, δ_0 is a Gaussian random variable with zero mean and variance of $\sigma(R)$. Thus the probability that δ_0 has a particular value in the range $[\delta_0, \delta_0 + d\delta_0]$ is given by

$$P(\delta_0, R)d\delta_0 = \frac{1}{\sqrt{2\pi}\sigma(R)} \exp(-\frac{\delta_0^2}{2\sigma(R)^2})d\delta_0 \tag{24}$$

This probability distribution in δ will translate to the probability $\mathcal{P}(S)dS$ of getting a given flux through (14) . Integrating this expression from S to infinity, we can find the cumulative probability $Q(S)$ for the flux to be larger than a value S. The *comoving* number density of protocondensates with fluxes larger than S will then be

$$N(S) = Q(S)(\frac{4\pi}{3}l^3)^{-1}(1+z)^{-3} \approx 2.39 \times 10^{-4} Q(S) \left(\frac{l(1+z)}{10Mpc}\right)^{-3} Mpc^{-3} \tag{25}$$

We can now calculate the expected flux from protoclusters in the CDM model at various redshifts and for a range of radii l and present the results as N versus S relations. But before we embark on this calculation (which is now straightforward) it is worthwhile to study the equation (20) closely and identify the range of values of θ which contribute to significant flux.

In order to calculate $Q(S)$ for a specified z and l, we have to first find the range of θ that gives a peak 21 cm flux greater than S. The quantity (S/A) is plotted as function of θ in figure 2. From this figure it is clear that - in general - two different ranges of θ satisfy this condition: a range of $[\theta_1, \theta_2]$ about the value $\theta = \pi$ and in addition a range $[\theta_3, 2\pi]$ with $\theta_2 < \theta_3$. (For values of S/A below certain limiting value, equation (20) has only one root; in which case, the relevant range is $\theta_1 < \theta < 2\pi$; see below). The first range corresponds to the case in which the protocluster is sufficiently near the epoch of turn around ($\theta = \pi$) so that the velocity width becomes small leading to a large flux. The second range corresponds to the case in which the density of the protocluster is tending to infinity because the structure is collapsing to zero radius. This, of course, is an artifact of the spherical model; in reality, the protocluster is likely to virialise and heat up (destroying the neutral hydrogen) much before this epoch. So the values of θ greater than some critical value, say θ_c, are unlikely to be of relevance in the physical context. We take $\theta_c = 3\pi/2$ which corresponds to the epoch at which the protocluster has collapsed to half its maximum radius. Hence we only need to concentrate on the range of values of θ less than θ_c.

While evaluating the contribution from near the epoch of turn-around we have to take into account the complication mentioned earlier; viz. that the smaller scale structures will themselves have a velocity width, say Δv_g. So even when Δv for the protocluster is very low (i.e., when $\Delta v \lesssim \Delta v_g$) the actual velocity width will still be about Δv_g. This leads to a lower limit on the velocity - and thus an upper limit on the flux S - near turn around for each z and l.

Given a range of values of θ which contribute a flux greater than S, we can find the corresponding range of δ_0, using (19) . So the probability $Q(S)$ of finding a flux greater than S, can be estimated by simply integrating (24) over the range of δ_0 corresponding to the range of $\theta_1 < \theta < \theta_2$ and $\theta_3 < \theta < 3\pi/2$. In performing this integration, we should take into account the fact that the co-moving radius R also depends on $\delta(z)$ - and hence on θ - via the relation $R = l(1+z)(1+\delta(z))^{1/3}$. We also adopt an effective power law

approximation for $\sigma(R) = \sigma(R_0)(R_0/R)^m$, where $R_0 = (9\pi^2/16)^{1/3} l(1+z) = 1.77 l(1+z)$ is the co-moving radius of a protocluster which has a proper radius l at turn around. We then have

$$Q(S) = \int_{\mathcal{R}} \frac{1}{\sqrt{2\pi}\sigma(R)} \exp(-\frac{\delta_0^2}{2\sigma(R)^2}) d\delta_0$$
$$= \frac{2Y}{3\sqrt{2\pi}} \int_{\mathcal{R}} d\theta (1-\cos\theta)^{1-m} (\theta - \sin\theta)^{(2m-1)/3} \exp(-\frac{Y^2}{2} \frac{(\theta-\sin\theta)^{4(1+m)/3}}{(1-\cos\theta)^{2m}}) \tag{26}$$

where

$$Y = \frac{0.4953(1+z)2^m}{\pi^{2m/3}\sigma(R_0)} \tag{27}$$

and the range of integration $\mathcal{R}$ is as described above. We can estimate $N(S)$ by substituting (26) in (25) .

3.3 Results and discussion

We shall now discuss the results of this computation. and compare it with the present and future sensitivities of various searches. For this, it is advisable to first fix the ideas regarding the actual numbers involved in such observational programs, in particular the GMRT.

We have summarised in Table 2 the numerical values of some of the relevant parameters of GMRT. (These have been worked out from the data in Swarup et al., 1991 and represent the theoretical expectations based on the design of GMRT). Note that GMRT will have an array of 30 antennas, 14 being configured as a central compact random array in an area of 1 square km, while the remaining being placed in three arms extending upto 14 km from the centre. We have given in Table 2 the following parameters: (1) the frequencies at which GMRT will search for redshifted HI, (2) the corresponding redshift which is being probed, (3) the field of view at various frequencies, (4) the angular resolution of synthesized beam, θ_s, when only the central compact array of antennas are used. (5) the expected rms (thermal) noise limits in the synthesized image for a point source being probed with a 100 kHz velocity resolution and 10 hour integration by the central array (6) the comoving volume $\mathcal{V}$ of the universe sampled per field, assuming a bandwidth of 16 MHz; this is defined by the relation

$$\mathcal{V} = d_A^2 d\Omega \frac{cdt}{dz} dz = \frac{4c^3}{H^3} \frac{(\sqrt{1+z}-1)^2}{(1+z)^{5/2}} d\Omega dz \tag{28}$$

where d_A is the angular diameter distance and we have set $\Omega = 1$. (7) the quantity $l(1+z)$ where l is the proper radius of the cloud which subtends the angle θ_s at the observer. These quantities are related by (7) .

Table 2 : Parameters and results for HI searches by GMRT

Frequency (MHz)	610	327	233	150
Redshift	1.33	3.34	5.1	8.47
Field of view (deg)	0.9	1.8	2.5	3.8
Resolution (arc min)	1.7	3.2	4.5	7.0
rms noise (mJy)	0.24	0.27	0.46	1.25
$\mathcal{V}$ (in 10^6 Mpc^3)	0.44	5.4	11.8	60.0
l(1+z) (Mpc)	2.06	5.84	9.4	16.58

Since the results depend sensitively on the redshift, it is preferable to discuss each redshift separately. We begin with the redshift $z = 3.34$, at which most of the present day searches for 21 cm emission are carried out. For this redshift, GMRT will have a resolution of about 3.2 arc min, corresponding to $l(1+z) \simeq 5.84 Mpc$ and an expected rms noise $\sigma_N \simeq 0.27 mJy$ (table 2). In searches which have already been carried out by Westerbork (Wieringa et al 1992) and by VLA (Uson et al 1991a,b) the rms noise level is about 5 times larger for similar resolutions in angular size and frequency. From table 1 we find that the collapsed fraction at this redshift is $f_{coll} = 0.3822$. We adopt $f_N = 0.5$ for the fraction of gas which is neutral in the collapsed objects and take $\Delta v_g = 300 Km^{-1}$ typical of 'galactic' scale clumps.

In figure 3a we give a plot of $N(S)$ against S for these parameters and for three values of $l(1+z) = 6, 8, 10$ Mpc. For these values of l the mass enclosed by a sphere of comoving radius R_0 is $3.5 \times 10^{14} M_\odot$, $8.3 \times 10^{14} M_\odot$ and $1.6 \times 10^{15} M_\odot$ respectively and the corresponding values of $\sigma(R_0)$ are 1.64, 1.27 and 1.03. The maximum flux that is obtained range from $0.7 mJy$ for $l(1+z) = 6 Mpc$ to $2.97 mJy$ for $l(1+z) = 10 Mpc$. We have also shown for comparison, in figure 3a, the expected rms noise level σ_N, of GMRT at this redshift (for 3.2 arc min resolution) and also the 5 σ_N level. (Note that there is an abrupt change in the nature of the $N(S)$ curve at some critical flux S_{cr}, with $N(S)$ dropping much more rapidly for $S > S_{cr}$. This is because, for $S < S_{cr}$ the range of integration $\mathcal{R}$ is $[\theta_1, 3\pi/2]$, while for $S > S_{cr}$ $\mathcal{R}$ changes to the ranges $[\theta_1, \theta_2; \theta_3, 3\pi/2]$; the contribution from the latter range declines sharply with S).

The flux in a pixel has to be above $1.4 mJy$ to be detectable at the 5 σ_N level when a resolution of 3.2 arc minute is used. For this resolution, the maximum flux obtained by our computation is below this value. However, one can get higher flux for higher values of l. The abundance of objects which have a flux above $1.4 mJy$ is $1.3 \times 10^{-8} Mpc^{-3}$ for $l(1+z) = 8 Mpc$ and $2.3 \times 10^{-8} Mpc^{-3}$ for $l(1+z) = 10 Mpc$. (These numbers should be compared with the abundance of rich Abell clusters which is about $5 \times 10^{-7} h_{50}^3 Mpc^{-3}$). One should also note that each field observed by GMRT at this redshift will sample a comoving volume of about $5.4 \times 10^6 h_{50}^{-3} Mpc^3$. *Hence it should be possible to detect these protoclusters with reasonable integration times and frequency resolutions after scanning about 8 fields with GMRT, provided the noise level does not increase drastically for a somewhat larger smoothening radius.*

Given the maximum fluxes estimated above and the rms noise levels of the instruments now in operation, it is not surprising that the searches carried out so far have only yielded null results. For the lone reported detection of a protocluster by Uson et al (1991b), the observed velocity width is $\Delta v \simeq 180 Kms^{-1}$ and the flux is about $11 mJy$. For this Δv and $l(1+z) = 10 Mpc$, the maximum flux is only about $4.6 mJy$ making it difficult to explain the detection of this object in the unbiased CDM models. (We will see in sections 3.4 and 4 that such an object is unlikely to exist in the biased CDM or HDM models as well).

Now consider the other redshifts which will be probed by GMRT. At $z = 1.33$, the GMRT synthesized beam corresponds to an $l(1+z) = 2.1 Mpc$. The collapsed fraction is $f_{coll} = 0.2354$ from table 1. It turns out that this radius contains too little mass to give a detectable signal above the noise. To explore the dependence on l, we have also tried a larger value of $l(1+z) = 10 Mpc$, which contains a cluster sized mass. Further there is considerable uncertainty in the neutral fraction at this redshift, since in CDM models with COBE normalisation, significant amount of the gas in the collapsed objects may have already turned into stars by this redshift. To handle this uncertainty, we have considered a range of f_N from 0.05 to 0.5. In figure 3b we have given N(S) versus S plots for $z = 1.33$, adopting the above values of l and f_{coll}, for the three values of $f_N = 0.05, 0.1$ and 0.5. The maximum flux which is obtained for these three values of f_N are $0.83 mJy$, $1.66 mJy$ and $8.32 mJy$ respectively. The abundance of objects expected above, say $1.5 mJy$, ranges from $2.1 \times 10^{-7} Mpc^{-3}$ for $f_N = 0.1$ to $1.4 \times 10^{-5} MPc^{-3}$ for $f_N = 0.5$. (Note that, for the

parameters specified in Table 2, the 5 σ_N level is about $1.2mJy$. However the rms noise level may be larger for the larger value of l adopted above.) In any case, it appears from the above numbers and figure 3b that observations at this redshift should place interesting limits on the nature of protoclusters.

At redshifts of 5.1 and 8.47 - which could also be probed by future observations - detectable protoclusters turn out to be extremely rare. For example, at $z = 5.1$, adopting $l(1+z) = 10Mpc$, $f_N = 0.5$ and $f_{coll} = 0.4265$, we find that the maximum flux is $1.75mJy$, where as the 5 σ_N level for detection by GMRT is a flux of about 2.3 mJy. We have shown in figure 3c a plot of $N(S)$ versus S for this case. Even the abundance of objects which have a flux just above the rms noise level of about $0.46mJy$, have $N(S) \simeq 3.8 \times 10^{-10} Mpc^{-3}$ for the above parameters.

One may wonder whether the more typical fluctuations with small density contrasts may be detectable at these redshifts due to the excess variance that they may contribute to the flux per pixel. (This is the second method of analysis mentioned in section 2). Using (26) , we find that the flux from the 1 σ density fluctuations at $z = 5.1$ and with $l(1+z) = 10Mpc$ is about $0.05mJy$. The expected rms noise from table 2 for a bandwidth corresponding to the Hubble velocity (which is relevant for small density contrasts; see equation (22)) and an integration time of 10 hours, is about 0.12 mJy. Therefore, excess variance will exceed the noise if the integration time is about 60 hours.

However, at $z = 8.47$, for $l(1+z) = 16.58Mpc$ (which corresponds to the synthesized beam size at this z), the excess variance will only be about $0.02mJy$, compared to the corresponding RMS noise of $0.30mJy$. So CDM models with COBE normalisation will be very difficult to probe at these redshifts.

It should be clear from the figures that $N(S)$ declines rather sharply for $S > S_{cr}$. This has the effect that $N(S)$ can change significantly for somewhat small changes in the σ_N of the instrument. Also note that we have calculated σ_N assuming a bandwidth of 100 KHz. On the other hand, the bandwidth corresponding to the minimum velocity width of $\Delta v_g \simeq 300 kms^{-1}$ will be $(2-3)$ times larger. It may be possible to use this fact and reduce σ_N in the search.

In all the above results, it turns out that detectable flux from protoclusters arises only when the protocluster is near turn around or when it has collapsed substantially. Further, the latter case (corresponding to $\theta_3 < \theta < (3\pi/2)$) contributes negligibly to $Q(S)$ compared to the first range (which corresponds to the protocluster being near turn around). Using this fact, one can obtain good analytical approximation to the numerical results presented above for the maximum detectable flux. (An analytical estimate of $Q(S)$ is, however, not correspondingly useful because of the presence of the exponential in the expression for Q(S); this makes the answer depend sensitively on the nature of the approximation employed). Near the turn around, we can write $\theta = \pi + \epsilon$, with $(\epsilon/\pi) \ll 1$. To the leading order in ϵ, (20) becomes

$$S = A(l,z)|\frac{\pi}{2\epsilon}|. \tag{29}$$

The velocity width, to the same order, is

$$\Delta v = 833\ Kms^{-1} \epsilon h_{50} \left(\frac{l(1+z)}{10Mpc}\right)(1+z)^{1/2} \tag{30}$$

The maximum flux is obtained for the minimum velocity width which corresponds to the condition $|\Delta v| \leq \Delta v_g$ evaluated at equality. This condition translates to

$$|\epsilon| \leq \frac{0.36}{(1+z)^{1/2}} h_{50}^{-1} \left(\frac{l(1+z)}{10Mpc}\right)^{-1} \left(\frac{\Delta v_g}{300Kms^{-1}}\right), \tag{31}$$

where we have adopted a typical galactic value of $\Delta v_g \sim 300 Kms^{-1}$. The maximum possible flux for a given z and l is obtained by setting $\Delta v = \Delta v_g$. We then find that:

$$S_{max} = 4.36A(l,z)(1+z)^{1/2}h_{50}\left(\frac{l(1+z)}{10Mpc}\right)\left(\frac{\Delta v_g}{300Kms^{-1}}\right)^{-1}$$
$$= \frac{3.739\,mJy}{g(z)}h_{50}^4\left(\frac{f_N}{0.5}\right)\left(\frac{f_b}{0.1}\right)\left(\frac{f_{coll}(z)}{0.5}\right)\left(\frac{l(1+z)}{10Mpc}\right)^3 f_{sig}\left(\frac{\Delta v_g}{300Kms^{-1}}\right)^{-1} \quad (32)$$

From the above equation, adopting $l(1+z) = 10Mpc$, $f_N = 0.5$ and f_{coll} as in table 1., we can estimate S_{max} at various redshifts. We get $S_{max} = 6.35mJy, 2.44mJy, 1.48mJy$ and $0.56mJy$ at redshifts 1.33, 3.34, 5.1 and 8.47 respectively. This compares reasonably with the numerical results discussed above.

3.4 Biased CDM models

We now briefly comment on the implications of possible biasing in CDM models, for the expected abundances and fluxes of protoclusters. In the first place. it must be stressed that the most natural interpretation of the COBE data would point to an unbiased model, at least at large scales. However, in models with power law type inflation in which gravitational waves can significantly contribute to the CMBR fluctuations, the level of density fluctuations indicated by the COBE quadrapole may be smaller than the value adopted above. In this case, $\sigma(R)$ at $R = 8h^{-1}Mpc$ may be less than unity, allowing one to make COBE results consistent with biased CDM models. The error bars on the CMBR quadrapole also allow a biasing factor of upto $b \sim 1.5$, even when there is negligible contribution from gravitational waves. Because of these reasons (and for the sake of completeness) we will examine the results for the 21 cm emission in the biased CDM models.

The introduction of the bias factor, $b = (\delta\rho/\rho)/(\delta j/j)$, where ρ and j are the mass and luminosity densities respectively on large scale, leads to two effects which are relevant for the computation of abundances and fluxes. First of all, with a bias parameter b greater than unity, $\sigma(R)$ is reduced by a factor b compared to the unbiased case. So each mass scale collapses at a later stage, and protoclusters which are about to become nonlinear are even rarer than the estimates made above (cf. equation (26)). However there is in principle an important trade off which is relevant for the detectability of protoclusters; namely that an enhanced number of small scale objects may form (per unit mass) in protocluster type environments compared to the general field. This, in turn, may lead to an enhanced HI content of the protocluster by a factor, say E, within a protocluster than estimated in equation (11) . Obviously this will enhance the flux by E. We need to take account of both the effects.

To incorporate first effect we have to replace $\sigma(R_0)$ in (26) by $[\sigma(R_0)/b]$ and also recompute the values of f_{coll} for the reduced σ. This is easily done. To incorporate the second effect, we need to estimate E which is more difficult. In order to estimate E one may use both theoretical ideas (Kaiser, 1985) and observations of present day clusters. Bardeen et al (1986) examine this question in some detail for the biased, $\Omega_0 = 1$, CDM model. For this model, they numerically estimate the degree of enhancement of the galactic number density within a typical Abell cluster forming now, compared to the general field. They assume $b = 2.5$ and get a value of $E \simeq (3-10)$ depending on how they smooth the density field (see their table 1). The observed properties of rich clusters can also be used to estimate E (eg. Dekel and Rees 1987). Suppose the number of galaxies per unit mass forming in a protocluster is indeed enhanced by a factor E compared to the field. Then when the cluster collapses, (and if the galaxies do not segregate from the mass), the excess density contrast in galaxies, $(\delta N/N)$, will also be a factor E larger than the mass contrast.

$(\delta M/M)$. So

$$E = \frac{\delta N/N}{\delta M/M} = (\frac{N_g}{n_b V_a})(\frac{M_{cl}}{\rho_b V_a})^{-1} = \frac{N_g < L >}{M_{cl}} \frac{\rho_c}{n_b < L >} \Omega_0 = \frac{(M/L)_{critical}}{(M/L)_{cluster}} \Omega_0. \quad (33)$$

Here N_g is the number of galaxies in a cluster of volume V_a and mass M_{cl} ; n_b the average galaxy number density in the field and ρ_b the background density of the universe. Also in (33) we have multiplied and divided by the average luminosity of a cluster galaxy $< L >$. Taking $(M/L)_{cluster} \simeq (200-400)h(M_\odot/L_\odot)$ and $(M/L)_{critical} \simeq 1500h(M_\odot/L_\odot)$ (Efstathiou et al 1988), we get $E \simeq (3.75 - 7.5)\Omega_0$. At a more fundamental level, it may be noted that the observation $(M/L)_{critical} > (M/L)_{cluster}$, needs to be explained in any theoretical model for structure formation. Biasing at large scales offers one possible explanation.

It is interesting to point out at this stage that arbitrarily large values of E cannot result from biasing. Recall that one may estimate the fraction of the mass in collapsed objects from Press-Schecter theory. Biasing can at most enhance this fraction to a value of unity. So E is constrained to a value such that $Ef_{coll} \lesssim 1$. We have also given in table 1 the f_{coll} estimated from Press-Schecter theory for $b = 1.5$. One then sees that E is constrained by $E \lesssim (2 - 3)$. We will return to this interesting constraint in a later work.

Adopting a value for $b = 1.5$ and a value of E such that $Ef_{coll} = 1$, we have recomputed the expected $N(S)$. This is shown in figure 4, for the case $z = 3.34$ and $l(1 + z) = 8Mpc$; we have also shown for comparison the corresponding unbiased case. In the biased case the number of expected objects with a flux $S \gtrsim 1.4mJy$ is $\sim 1.5 \times 10^{-8} Mpc^{-3}$, for $l(1 + z) = 8Mpc$. This is similar to the abundance obtained in the unbiased case. So the decrease in probability due to $b > 1$ has been virtually canceled out by the increase in the effective collapsed fraction Ef_{coll}.

In the biased case, one can obtain - in principle - much larger fluxes. For example fluxes greater than $10mJy$ can be obtained with $Ef_{coll} = 1$, if we take $l(1 + z) = 10Mpc$, $f_N = 0.5$ and a minimum $\Delta v = 180Kms^{-1}$ as the relevant parameters for the object reported by Uson et. al (1991b). *However, this feature is more than offset by the fact that the number density of objects with a flux greater than this value turns out to be negligibly small*: ranging from $N \simeq 10^{-14} Mpc^{-3}$ for $b = 1.5$ to $N \simeq 10^{-12} Mpc^{-3}$ for $b = 1.3$. So, even with biasing, it is highly unlikely that we will detect objects with such large fluxes.

4. The 21 cm flux in the HDM model

A dark matter particle which is still relativistic when it decouples is called hot dark matter. In these models, the large free streaming velocity wipes out the fluctuations on small mass scales and the processed spectrum has maximum power at cluster scales. Massive protoclusters are the first structures to collapse in this scenario. This collapse is expected to preferentially occur along one axis leading to pancake like structures first; the gas in pancakes cools and later fragments to form galaxies. In this model, each cluster is supposed to have gone through a phase when the gas is in the form of a cooled neutral hydrogen pancake. It is these pancakes that one would like to detect by their 21 cm emission.

A typical example of a HDM candidate is a massive neutrino with a mass of $m_\nu \simeq 91.5\Omega_\nu h^2 eV$, where Ω_ν is the density of neutrinos in units of the critical density. For $\Omega_\nu = 1$ and $h = 0.5$, the neutrino mass is constrained to be $m_\nu \lesssim 25eV$. (Note that, for the $\Omega = 1$ model which we are considering, h is constrained to be less than about 0.6). In the HDM models the power per logarithmic interval in k is given by (cf. Bond and Szalay 1983)

$$\Delta^2(k) = \frac{k^3 P(k)}{2\pi^2} = \frac{Ak^4}{2\pi^2} \exp[-4.61(k/k_{FS})^{3/2}] \tag{34}$$

where $k_{FS} = 0.16 Mpc^{-1}(m/30eV)$, and A is a normalisation constant. From COBE quadrapole data we can determine the value of the normalisation constant to be $A = (24h^{-1})^4 Mpc^4$ as before. From (34) we can calculate the scale, say k_m, for which the power in density fluctuations has a maximum. This is the scale which will collapse first, at a redshift which depends on the magnitude of $\Delta(k)$ at k_m. A simple calculation gives $k_m = 0.69 k_{FS}$ corresponding to a mass scale $M_c \simeq 3.76 \times 10^{14} h_{50}^2 M_\odot$ and

$$\Delta_{max} = \Delta(k_m) = 1.4(\frac{h}{0.5})^{-2} \left(\frac{m_\nu}{25eV}\right), \tag{35}$$

Note that the COBE results (which fix A) have completely eliminated any uncertainty in this value. We have seen earlier that the collapse of structures occur when the linear density contrast (extrapolated to the present) is of order unity. Using the spherical model for nonlinear evolution we have from (5)

$$(1 + z_{coll}) \approx \frac{n\Delta_{max}}{1.68} = 0.83 n h_{50}^{-2} (\frac{m_\nu}{25eV}) \tag{36}$$

for an $n\sigma$ fluctuation, even at the scale which has the maximum power. So the COBE normalisation implies that the first structures in HDM theory will typically begin to go non-linear only at the present epoch. *This, in turn, implies that the high redshift. cluster scale, pancakes of HI that are being looked for in the searches will be quite rare in the HDM model.* The expected co-moving number density N_p of such objects, at any redshift z can be easily estimated. The Gaussian statistics for the linear density field implies that the abundances of structures of mass scale M_c will be

$$\begin{aligned} N_p &\simeq \frac{\rho_0}{M_c} \exp[-\frac{n^2}{2}] \\ &\approx 1.86 \times 10^{-4} h_{50}^2 Mpc^{-3} \exp[-0.73(1+z)^2 h_{50}^4 m_{25}^{-2}] \end{aligned} \tag{37}$$

From (37) we have $N_p \simeq 3.5 \times 10^{-6} Mpc^{-3}$ at $z = 1.33$ and $N_p \simeq 2.15 \times 10^{-10} Mpc^{-3}$ at $z = 3.34$. So, except at a low redshift of $z = 1.33$, the detection of such pancakes will be an extremely rare event in protocluster searches, if HDM theories are correct.

Note that in the earlier versions of HDM the normalisation constant could be arbitrarily chosen so as to have sufficient number of pancakes collapsing at high redshifts, in order to explain high z quasars and galaxies. But with the advent of COBE results one no longer has the freedom to choose a larger value for A. It should also be added here that any gravitational wave contribution to the CMBR fluctuations detected by COBE, will further reduce the probability for collapse of pancakes at high z. One sees here the extent to which COBE has proved useful in constraining HDM models, and indirectly, the expected 21 cm signals. This is a significant departure from the pre-COBE days when HDM models were considered the main provider of neutral hydrogen pancakes at high redshifts.

The flux from a pancake with mass M_c, and a neutral fraction $f_N = 0.5$, is about $1.9mJy(\Delta v/1000kms^{-1})^{-1}$ at $z = 1.33$ and about $0.44mJy(\Delta v/1000kms^{-1})^{-1}$ at $z = 3.34$. So the expected flux from a pancake may not pose as serious a problem for detectability as their expected abundance at high redshifts. Also note that, at z=5.1, the excess variance in the flux per pixel is about 0.08 mJy which is comparable to the corresponding value in the CDM model and hence will be detectable with sufficiently long integration time. But the fact that the first collapsed structures in HDM models form only at low z, renders the HDM model itself very unattractive as a theory of structure formation.

The following point needs to be stressed: In the above argument, we have applied the result of spherical model to the peak scale without explicitly taking into account of the effects of asymmetry in protocluster collapse. Due to asymmetric collapse, the short axis of the protocluster could turn around at high redshift, while the long axis does so only at a low z. It might seem at first that this fact might provide a way out of the above bound: Could it be that the long axis collapses only at low z but the pancake collapses along the short axis at higher z, due to asymmetry in the initial density field ? This effect, however, cannot play any significant role when the peak power is low. Notice that the density in typical region of the universe will increase to nonlinear values if the pancake formation (due to the collapse along the short axis) takes place at a significant rate. This, in turn, will increase the rms power at the corresponding scales to values far higher than unity. Hence, significant production of pancakes cannot occur as long as the rms power at all scales remains less than the critical value, $\delta_c = 1.68 \simeq 1$. In other words, collapse along short axis as well as production of significant amount of pancakes can take place only *after* the peak scale has gone nonlinear. The above calculation shows that this occurs at a very low redshift.

For the sake of completeness, it may be mentioned that we have also analysed mixed models in which both HDM and CDM candidates are present. They do not provide any improvement over the CDM models studied in section 3 as regards the flux or abundance.

5 Summary

In this paper we have been concerned with the predictions from the CDM and HDM models, for the detectability of protocondensates using redshifted 21 cm emission. For this purpose we have calculated the expected flux and abundances of protocondensates in these models for a number of redshifts. These results have been compared with the capabilities of various present and planned searches for neutral hydrogen.

It has been generally believed in the past that the most promising sources of HI are the cluster size objects which have collapsed into pancakes. These are thought to occur naturally in HDM models; however the COBE results, by fixing the normalisation of the power spectrum, have ruled out this possibility at $z \gtrsim 2$.

Cluster mass objects collapse at a low redshift in the CDM models as well. However there exists another source of HI in these models, resulting from the collapse and cooling of gas into smaller mass clumps at sufficiently high redshifts. Previous studies of the detectability of HI condensates in CDM models have tended to neglect this feature. The present work shows that protoclusters consisting of smaller mass HI clumps, may be detectable, in sufficient numbers (about $10^{-8} Mpc^{-3}$) and with large enough flux (1.5 - 3 mJy) at redshifts $z \simeq 3.3$. The planned searches with GMRT, for example, are likely to detect these objects with reasonable integration times. At lower redshifts ($z \simeq 1.3$), the major uncertainty is the fraction of the collapsed gas which remains as HI. If this fraction is about 0.1, one should be able to detect protoclusters at a flux level of $1.5 mJy$ and abundance of about $10^{-7} Mpc^{-3}$. In the redshift range around $z \simeq 5$, *individual* protocondensates will not be detectable. However, the excess variance due to fluctuations with small density contrasts will be detectable with somewhat large (say, about 60 hours) integration time. At still higher redshifts, it would be virtually impossible to see any signal with even such large integration time. [This is in agreement with the results obtained by Scott and Rees (1990) at $z = 8$].

We have also looked at the possible effect of biasing in the CDM model. In this case the predicted fluxes are larger but the abundance at any flux level depends sensitively on the value of the bias parameter b.

The object reported by Uson et al. (1991b) at $z = 3.4$, with a flux of about $10 mJy$, is extremely unlikely to arise in *any* of the models. It cannot be a Zeldovich pancake, since the predicted abundance of such pancakes is about $10^{-10} Mpc^{-3}$ in the HDM models normalised using COBE. It is rare in CDM models as well because of the following reason: To explain the high flux of this object one needs an enhanced fraction of collapsed objects in the protocluster and hence a biasing in the model. This, however, makes the expected abundance very small, ranging from $10^{-12} Mpc^{-3}$ for $b = 1.3$ to $10^{-14} Mpc^{-3}$ for $b = 1.5$. If the detection of this object is confirmed it could pose a serious problem for all models.

The major uncertainty in our work arises from the lack of knowledge about the ionisation and the thermal history of the gaseous component. We plan to return to this question in a later publication.

Acknowledgements

We thank Pramesh Rao, C.R.Subrahmanya, Ravi Subrahmanyan and Govind Swarup for helpful conversations.

References

Bardeen, J.M., Bond, J.R., Kaiser, N & Szalay, A.S., 1986. Astrophy. J., **304**, 15.
Blumenthal, G.R., Faber, S.M., Primack, J.R. & Rees, M.J., 1984. Nature, **341**, 517.
Bond, J.R. & Szalay, A.S., 1983, Astrophys. J., **274**, 443.
Cowie, L.L., 1988. *The Post Recombination Universe* (eds. Kaiser, N., Lasenby, A.N.) (Kluwer Academic Publishers, Dordrecht), p1.
Davis, M., Efstathiou, G., Frenk, C.S. & White, S.D.M., 1985. Astrophys. J., **292**, 371.
Dekel, A. & Rees, M.J., 1987. Nature, **326**, 455.
Efstathiou, G., 1992. Mon. Not. R. Astr. Soc., **256**, 43p.
Efstathiou, G., Ellis, R.S. & Peterson, B.A., 1988. Mon. Not. R. astr. Soc., **232**, 431.
Gunn, J.E. & Peterson, B.A., 1965. Astrophys. J., **142**, 1633.
Hogan, C.J. & Rees, M.J., 1979. Mon. Not. R. Astr. Soc., 188, 791.
Lanzetta, K.M., Wolfe, A.M., Turnshek, D.A., Lu, L., McMahon, R.G. & Hazard, C., 1991. Astrophys. J. Suppl., **77**, 1.
Kaiser, N., 1985. Astrophys. J., **284**, L9.
Miralda-Escude, J. & Ostriker, J.P., 1990. Astrophys. J., **350**, 1.
Padmanabhan, T. & Narasimha, D., 1992. Mon. Not. R. Astr. Soc. (in Press).
Peebles, P.J.E., 1983. Astrophys. J., **263**, L1.
Peebles, P.J.E., 1980. *Large Scale Structure of the Universe* (Princeton University Press, Princeton). Press, W.H., & Schecter, P., 1974. Astrophys. J., **187**, 425.
Scott, D. & Rees, M.J., 1990. Mon. Not. R. Astr. Soc., **247**, 510.
Smoot, G.F et al. (1992) Astrophys. J., **396**, L1.
Spitzer, L., 1978. *Physical Processes in the Interstellar Medium*, (Wiley - Interscience : New York).
Subrahmanyan, R., 1989. PhD. Thesis, (Indian Institute of Science, Bangalore).
Subrahmanyan, R., & Anantharamaiah, K.R., 1990. J. Astrophys. Astron., **11**, 221.
Subrahmanyan, R., & Swarup, G., 1990. J. Astrophys. Astron., **11** 237.
Subramanian, K. & Swarup, G., 1992. Nature, **359**, 512.
Sunayaev, R.A. & Zeldovich, Ya.B., 1972, Astron. Astrophys., **20**, 189.
Sunayaev, R.A. & Zeldovich, Ya.B., 1974, Mon. Not. R. Astr. Soc., **171**, 375.
Swarup, G., 1984. *Gaint Metre-Wavelength Radio Telescope - Proposal*, Radio Astronomy Centre, TIFR, India.
Swarup, G., Ananthakrishnan, S., Kapahi, V.K., Rao, A.P., Subrahmanya, C.R. & Kulkarni, V.K., 1991. Current Science, **60**, 95.
Turnshek, D.A., Wolfe, A.M., Lanzetta, K.M., Briggs, F.H., Cohen, R.D., Foltz, C.B., Smith, H.E. & Wilkes, B.J., 1989. Astrophys. J., **344**, 567.
Uson, J.M., Bagri, D.S. & Cornwell, T.J., 1991a, Astrophys. J., **377**, L85.
Uson, J.M., Bagri, D.S. & Cornwell, T.J., 1991b. Phys. Rev. Lett., **67**, 3328.
Wieringa, M.H., de Bruyn, A.G. & Katgert, P., 1992. Astron. Astrophys., **256** 331.
Wolfe, A.M., 1989. *The Epoch of Galaxy Formation* (eds. Frenk, C.S., Ellis, R.S., Shanks, T., Heavens, A.F., Peacock, J.A.) (Kluwer, Dordrecht), p101.
Wolfe, A.M., Turnshek, D.A., Smith, H.E. & Cohen, R.D., 1986. Astrophys. J. Suppl., 61, 249.

Figure Captions

Fig. 1. A plot of $\sigma(R)$ versus R for the CDM models with the bias parameter $b = 1$ (solid line) and $b = 1.5$ (dashed line).

Fig. 2. A plot of S/A versus θ.

Fig. 3a. The abundance $N(S)$ of protoclusters with a flux greater than S at $z = 3.34$ for $l(1+z) = 10Mpc, 8MPc$ and $6Mpc$. We also marked the $1\sigma_N$ and $5\sigma_N$ noise levels for detection by GMRT.

Fig. 3b. $N(S)$ versus S at $z = 1.33$ for $f_N = 0.05, 0.1$ and 0.5. We also marked the $5\sigma_N$ noise level for detection by GMRT.

Fig. 3c. $N(S)$ versus S at $z = 5.1$ for $l(1+z) = 10Mpc$ and $f_N = 0.5$. We also marked the rms noise level for detection by GMRT.

Fig. 4. $N(S)$ versus S for a biased CDM model with $b = 1.5$ at $z = 3.34$. We have adopted $l(1+z) = 8Mpc$ and also shown the corresponding unbiased case for comparison. The $5\sigma_N$ noise level for detection by GMRT has been marked in the figure.

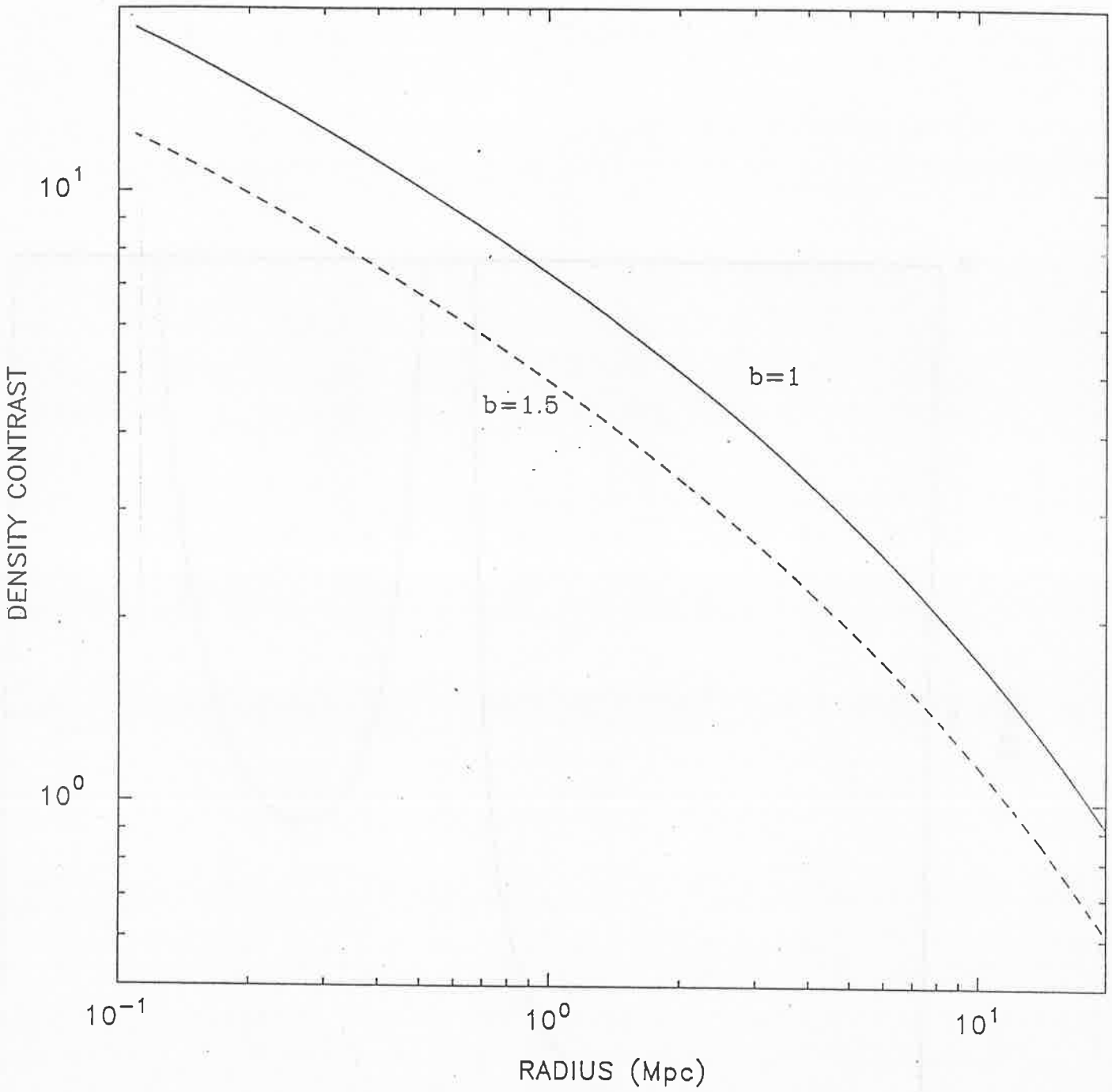

FIG 1

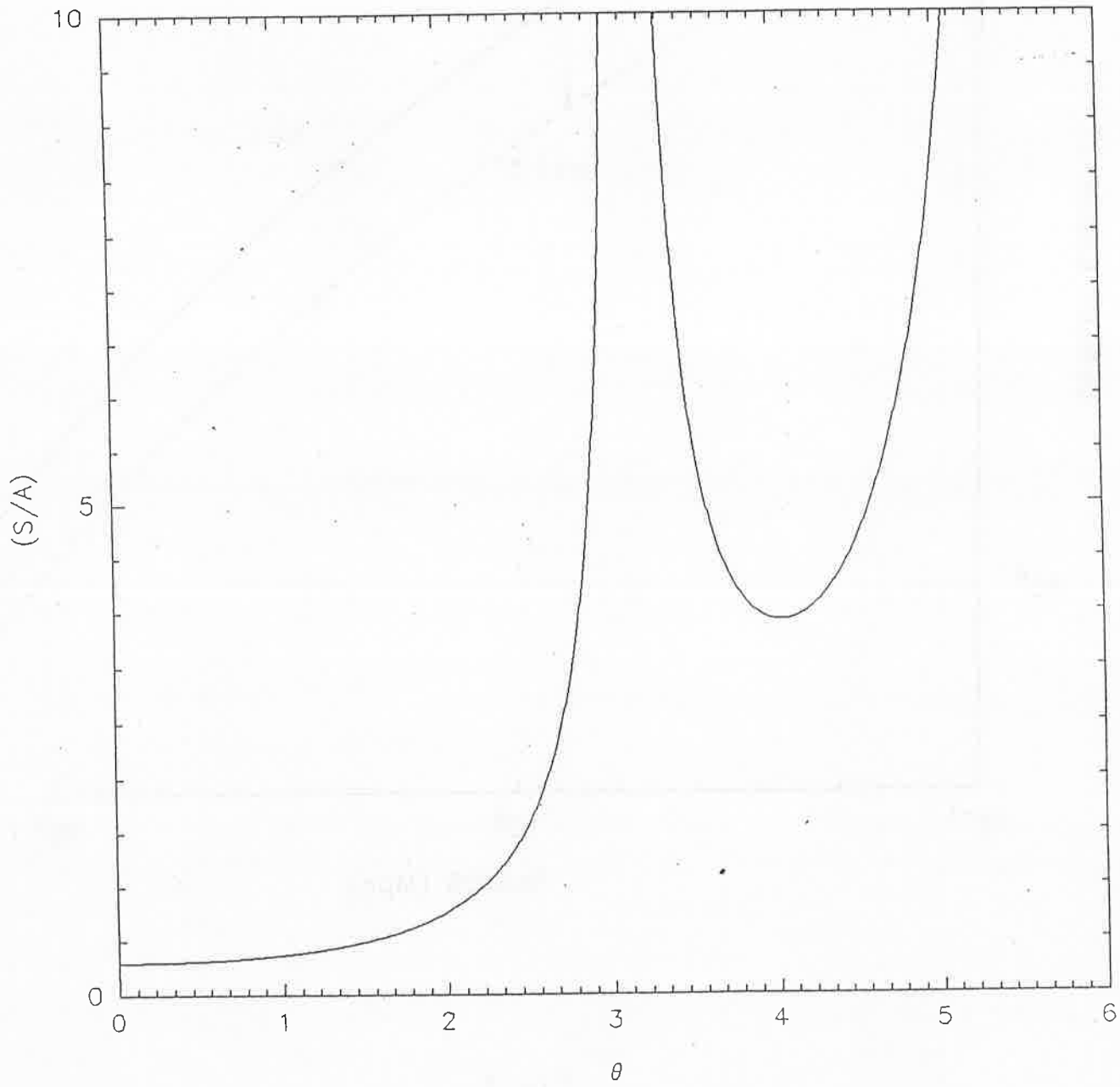

FIG. 2

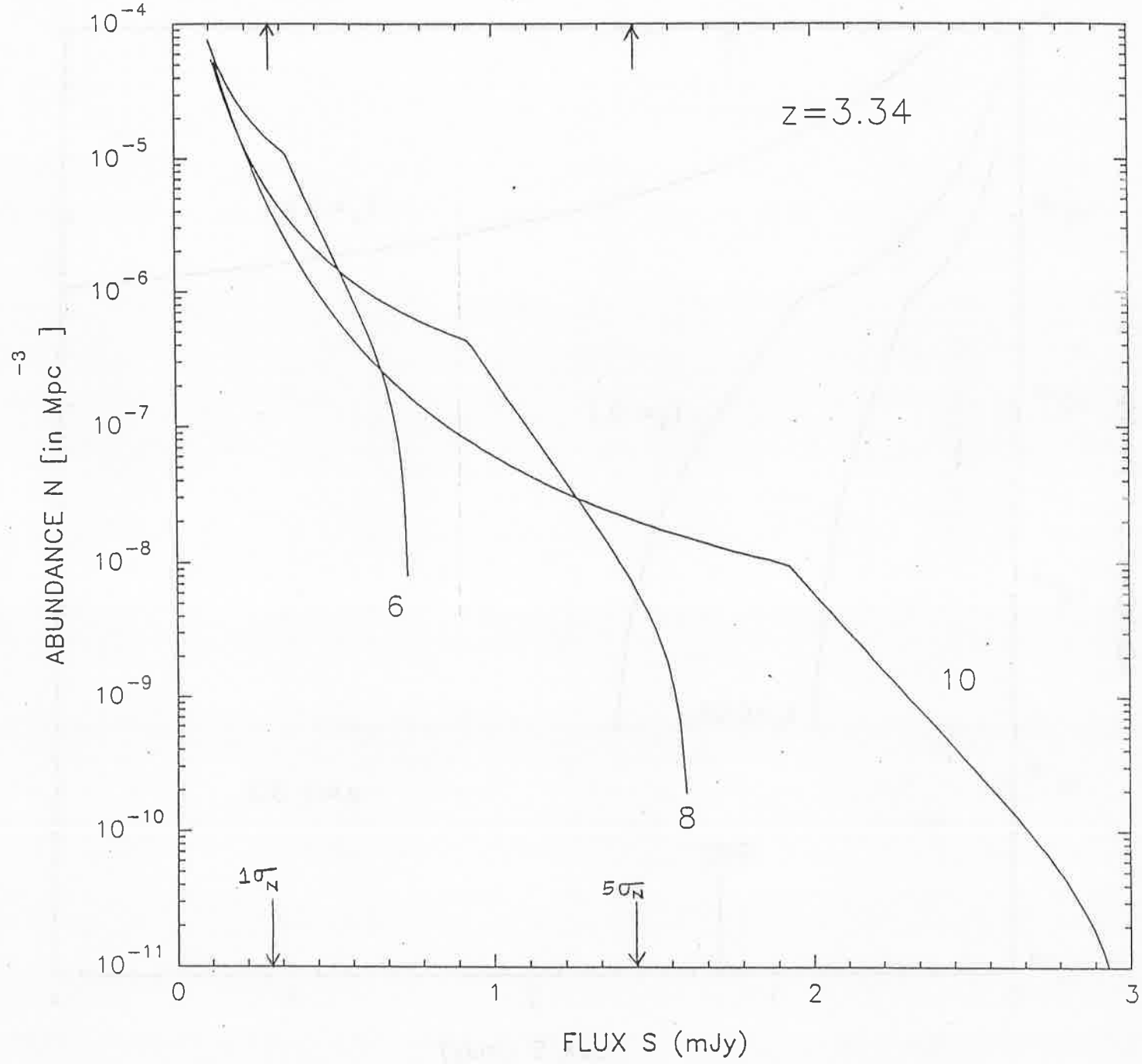
z=3.34
6
8
10
$1\sigma_N$
$5\sigma_N$
ABUNDANCE N [in Mpc^{-3}]
FLUX S (mJy)
10^{-4}
10^{-5}
10^{-6}
10^{-7}
10^{-8}
10^{-9}
10^{-10}
10^{-11}
0
1
2
3

FIG. 3(a)

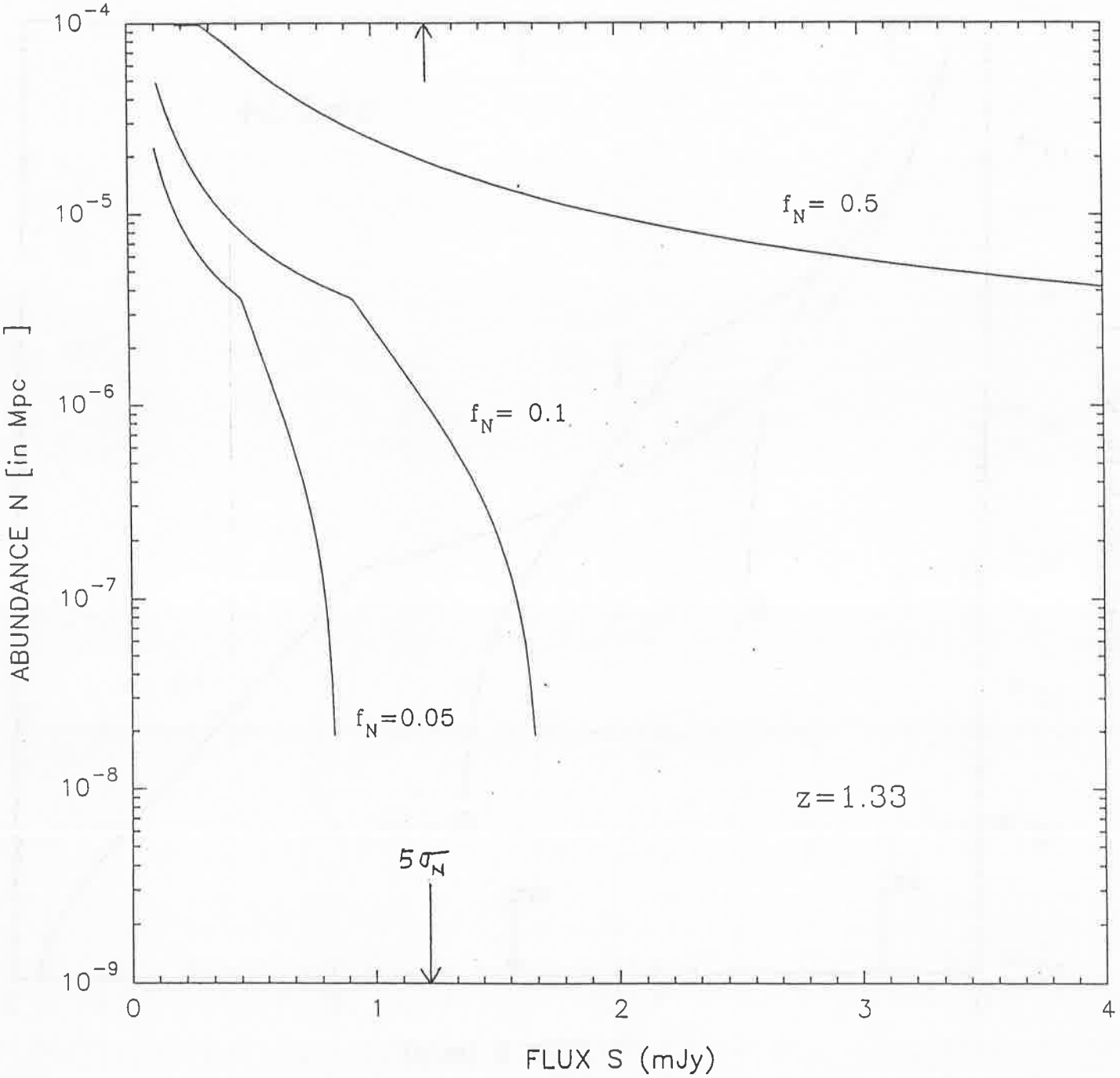
10^{-4}
10^{-5}
10^{-6}
10^{-7}
10^{-8}
10^{-9}
ABUNDANCE N [in Mpc]
f_N= 0.5
f_N= 0.1
f_N=0.05
z=1.33
$5\sigma_N$
0
1
2
3
4
FLUX S (mJy)

FIG. 3(b)

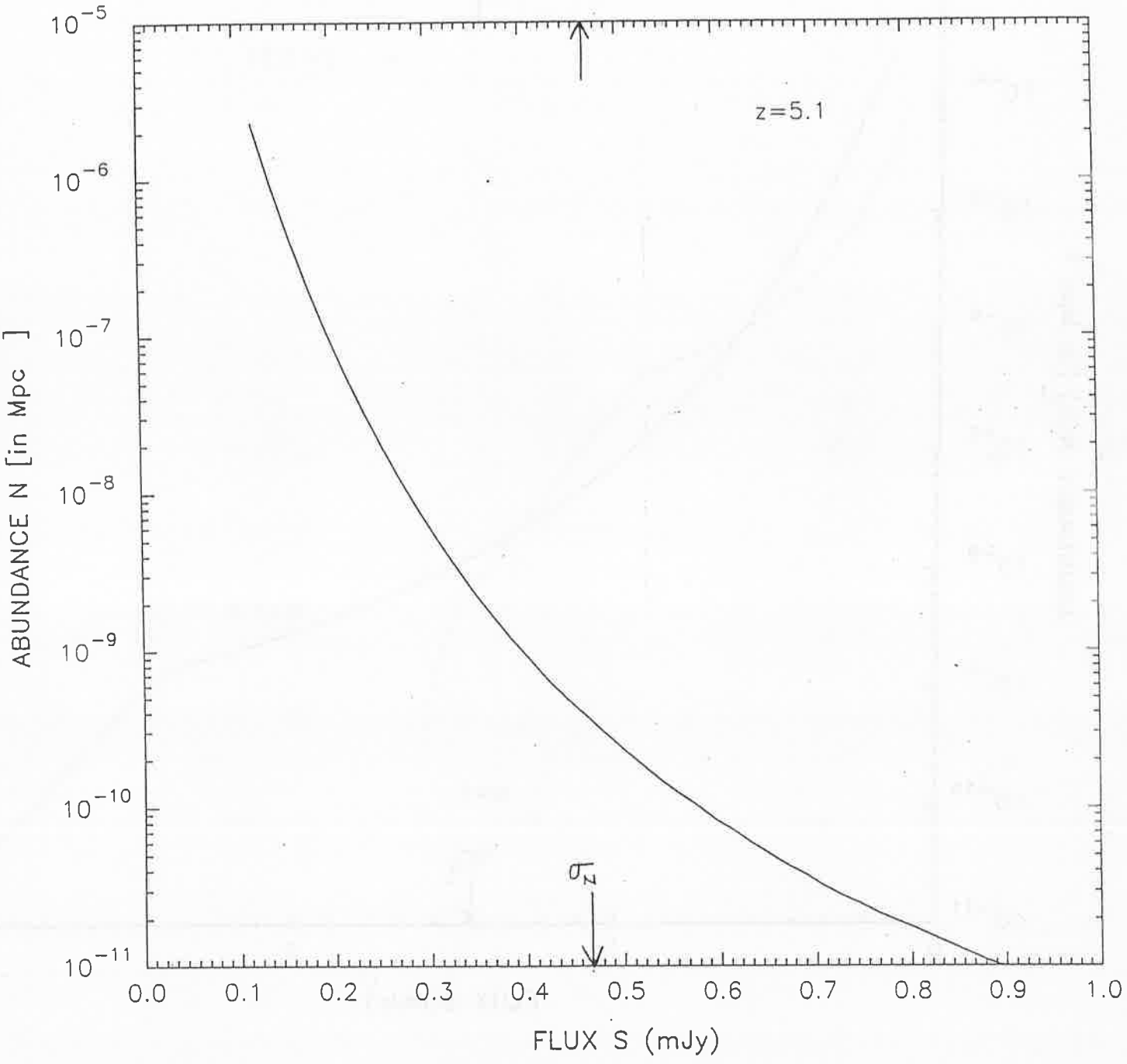
z=5.1
10^{-5}
10^{-6}
10^{-7}
10^{-8}
10^{-9}
10^{-10}
10^{-11}
ABUNDANCE N [in Mpc^{-3}]
σ_z
0.0
0.1
0.2
0.3
0.4
0.5
0.6
0.7
0.8
0.9
1.0
FLUX S (mJy)

Fig. 3(c)

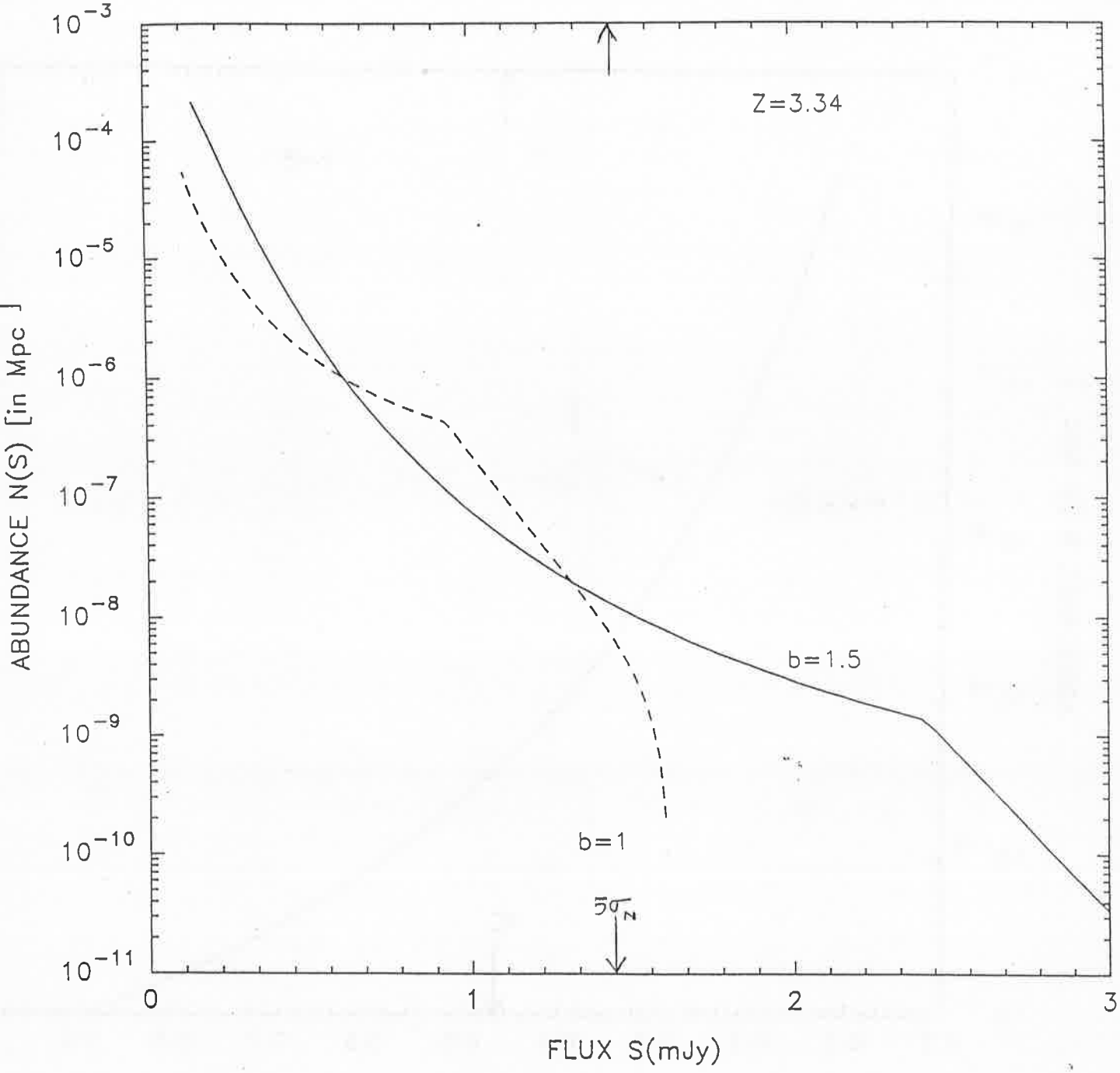
Z=3.34
b=1.5
b=1
5σz
ABUNDANCE N(S) [in Mpc^-3]
FLUX S(mJy)
10^-3
10^-4
10^-5
10^-6
10^-7
10^-8
10^-9
10^-10
10^-11
0
1
2
3

FIG. 4